08

# Femtosecond laser synthesis of spherical nanoparticles of molybdenum disulfide and molybdenum oxide for photothermal therapy

© A.S. Chernikov, D.A. Kochuev, R.V. Chkalov, M.A. Dzus, K.S. Khorkov

Vladimir State University, 600000 Vladimir, Russia e-mail: khorkov@vlsu.ru

Received December 25, 2024 Revised May 7, 2025 Accepted May 7, 2025

The paper presents the results of femtosecond laser ablation and fragmentation of molybdenum disulfide and molybdenum oxide nanoparticles in ethanol and acetone. The photosensitized nanoparticles obtained were studied using scanning electron microscopy and Raman spectroscopy. The average size of nanoparticles after laser ablation was about 36 nm and 57 nm in ethanol and acetone, respectively. Laser fragmentation has made it possible to reduce the average size of nanoparticles in an ethanol solution to 20 nm, while sedimentation and oxidation of ablated nanoparticles are observed. Optical density spectra of solutions of  $MoO_{3-x}$  and  $MoS_2$  nanoparticles in ethanol and graphs of the dependence of temperature changes on irradiation time and transmitted radiation power on time are presented.

**Keywords:** laser ablation, laser fragmentation, molybdenum disulfide, photosensitized nanoparticles, hyperthermia, photothermal response.

DOI: 10.61011/TP.2025.08.61739.468-24

## Introduction

Nanomaterials with the photothermal effect are widely studied now. Compounds that have significant absorption in the red spectrum range are applied as photosensitizers, thereby making it possible to achieve higher efficiency of photodynamic effect by increase of a depth of penetration of light into biological tissues. Tumor cells are more sensitive to heat and, therefore, the received heat can be used in photothermal therapy for burning defect cells without damaging to other surrounding healthy tissues [1-4]. Molybdenum disulfide and molybdenum oxide nanoparticles (MoS<sub>2</sub>, MoO<sub>3-x</sub>) can be effectively used in biomedicine due to effective photothermal conversion and biological safety [5–8]. These photosensitized nanoparticles can be obtained by various chemical methods, ultrasonic action, etc. [9-11]. However, using laser radiation has several advantages and makes it possible to use various media for synthesis of the nanoparticles [12,13].

Femtosecond laser synthesis of the nanoparticles is one of the advanced fields in developing of technologies of optoelectroncis, biophotonics and theranostics. Using ultrashort laser pulses provides high flexibility of functionalization of nanoobjects, processing of a wide range of materials with precise dosing of transferred energy to exclude inertial thermal processes, which is an advantage compared to impact by longer laser pulses [14–16]. When using femtosecond laser radiation, it is possible to minimize interaction between radiation and a plasma as well as to reduce heat-affected areas, forming spherical particles and surface structures [17,18]. Pulsed laser ablation in liquids makes it possible to synthesize various nanomaterials with

unique chemical properties, various morphology and sizes. Laser methods of synthesis provide obtaining stable colloidal free-impurity solutions. The size of the synthesized particles is determined by parameters of laser effect, the medium type and properties of the initial material. Thus, it is possible to synthesize pure colloidal solutions that will be suitable for further application in biological technologies.

The aim of the present study is to investigate processes of obtaining molybdenum-based nanoparticles by femtosecond laser radiation, which have effective absorption in the near-IR spectrum range.

## 1. Materials and experimental diagrams

The molybdenum disulfide nanoparticles were synthesized by pulsed laser ablation in the liquid medium. The target was a molybdenum disulfide crystal (MoS<sub>2</sub>), while the liquid media were ethyl alcohol (ethanol) and chemically pure acetone. They were synthesized according to the diagram of Fig. 1. A source of radiation in the experiments was a femtosecond laser system TETA-10 (Avesta-Project, Troitsk, the Russian Federation) with the following parameters: the pulse duration of 280 fs, the pulse energy of  $100\,\mu\text{J}$ , the wavelength of  $1030\,\text{nm}$ . A treated area was a square  $5\times 5\,\text{mm}$ , the velocity of laser beam scanning was  $100\,\text{mm/s}$ , the number of lines per millimeter was 20, the number of repetitions was 60, the layer of the liquid medium above the target was about 8 mm.

The produced colloidal solutions were again subjected to laser irradiation using a technique of pulse laser fragmentation in the liquid medium. Fig. 2 shows a diagram of laser

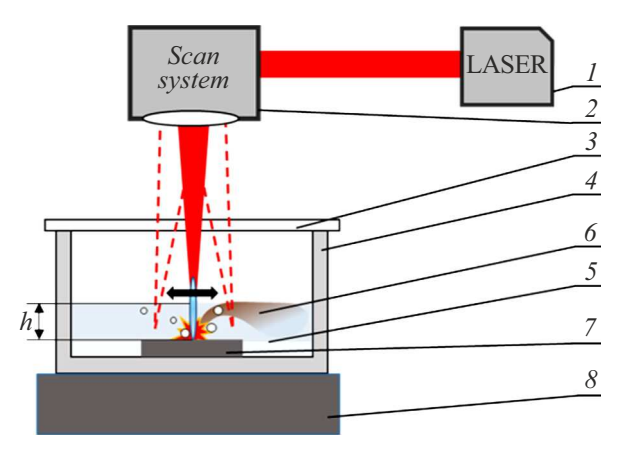


**Figure 1.** Schematic representation of the process of laser ablation in the liquid medium: I — the source of laser radiation (LR), 2 — the flat-field lens with galvanometric scanners, 3 — the window for inputting laser radiation, 4 — the quartz cuvette, 5 — the liquid medium, 6 — the nanoparticles being formed, 7 — the target, 8 — the vertical linear translator, h — the LR path length in the liquid medium.

fragmentation in the liquid medium and an image of an test tube with the colloidal solution.

A magnetic anchor was placed at the bottom of the test tube with the colloidal solution, the ampoule was placed in a special holder arranged on a magnetic mixer. During laser irradiation, mixing is performed by rotating the magnetic anchor using the mixer. A position of the focus and the effected area were tuned by means of a coordinate stage. Laser fragmentation of the colloidal solutions  $MoS_2$  was carried out at the same value of the energy as in the case of laser ablation  $(100\,\mu\mathrm{J})$  and the duration of the fragmentation process ranged from 10 to 70 min. At the same time, the beam was not in a stationary position and the scanning was along a pre-defined trajectory (a circle of the diameter of 4 mm and with X-shaped filling, the density of the filling lines was  $20\,\mathrm{lines/mm}$ ).

# Results of laser treatment and discussion thereof

Upon completion of the laser ablation synthesis process, the colloidal solutions had a brown shade. With the same modes of laser impact, the mass of the material removed for the laser ablation stage with the energy of  $100\,\mu J$  in ethanol is  $\sim 0.9\,mg$  (the concentration of  $0.18\,mg/ml)$  and  $\sim 0.65\,mg$  (the concentration of  $0.13\,mg/ml)$  in acetone.

Using the scanning electron microscope (SEM), images of the  $MoS_2$  nanoparticles as a result of laser ablation in ethanol were obtained, so were the histograms of size distribution of the nanoparticles based on a series of the SEM images. The typical SEM images are shown in Fig. 3.

The typical SEM image of the  $MoS_2$  nanoparticles produced during laser radiation in acetone as well as the histograms of size distribution of the  $MoS_2$  nanoparticles are shown in Fig. 4.

The size of the  $MoS_2$  nanoparticles produced as a result of laser ablation in ethanol is within the range from 10 to 120 nm, the average size of the nanoparticles is  $\approx 36$  nm.

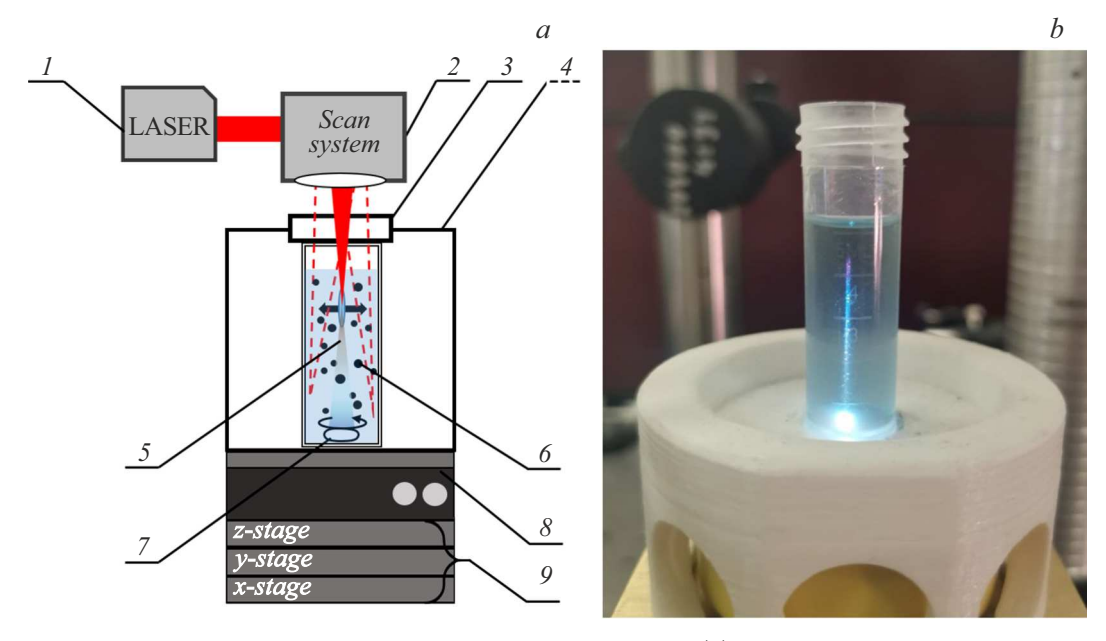


**Figure 2.** Diagram of the process of laser fragmentation in the liquid medium (a) and the image of the test tube with the colloidal solution (b): I — the laser system, 2 — the galvanic scanner; 3 — the window for inputting laser radiation; 4 — the dust-protection box; 5 — generation of the supercontinuum; 6 — the colloidal solution; 7 — the magnetic anchor; 8 — the magnetic mixer; 9 — the coordinate stage.

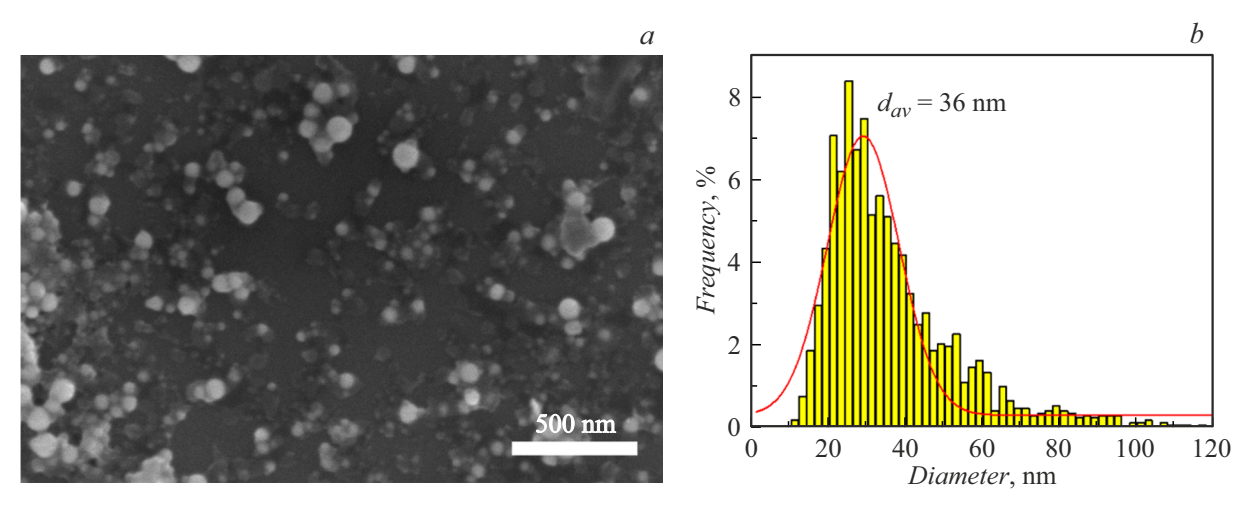


**Figure 3.** Typical SEM image of (a) and the histogram of size distribution of (b) the MoS<sub>2</sub> nanoparticles produced as a result of laser ablation in ethanol.

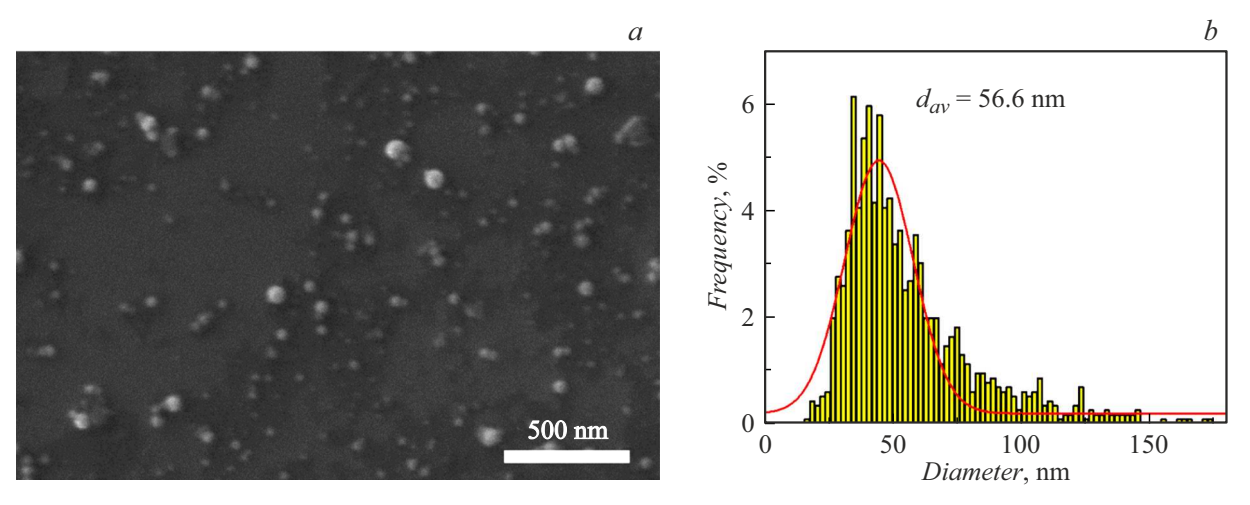
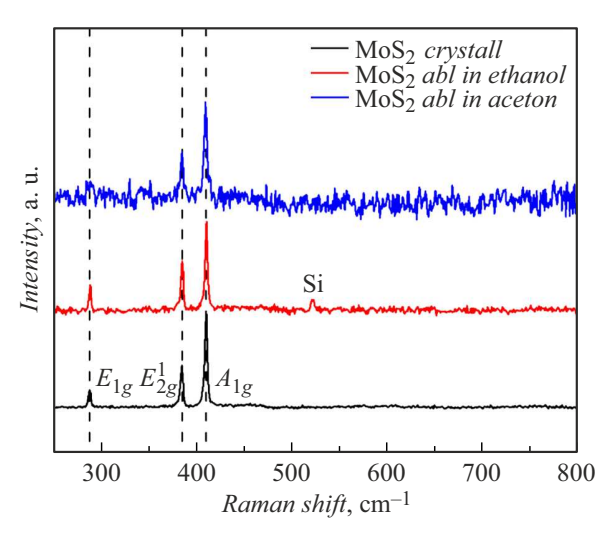


Figure 4. Typical SEM image of (a) and the histogram of size distribution of (b) the MoS<sub>2</sub> nanoparticles produced as a result of laser ablation in acetone.

The nanoparticles produced in acetone have the average size of  $\approx 57\,\text{nm}.$ 

The Raman scattering (RS) spectra of the synthesized solutions were measured in a back scattering geometry using the probe nanolaboratory NTEGRA Spectra (NT-MDT, Zelenograd, the Russian Federation). To study the samples, a diode-pumped solid-state laser at the wave of 473 nm was used as a source of excitation. Fig. 5 shows the RS spectra of the initial MoS2target and the nanoparticles produced during laser ablation in ethanol and in acetone. The samples were prepared for RS spectroscopy by depositing  $30\,\mu l$  of the colloidal solution of the nanoparticles to a surface of the silicon plate.

In case of the RS spectra, the nanoparticles have the modes  $E_{1g}$  (288 cm<sup>-1</sup>),  $E_{2g}^1$  (385 cm<sup>-1</sup>),  $A_{1g}$  (410 cm<sup>-1</sup>), which belong to the 2*H*-MoS<sub>2</sub> phase. It indicates that the MoS<sub>2</sub> phase is preserved in the produced colloidal solutions and no oxidation is observed.



**Figure 5.** RS spectra of the initial  $MoS_2$  target (the black line) and the nanoparticles produced as a result of laser ablation in ethanol (the red line) and in the acetone (the dark blue line).

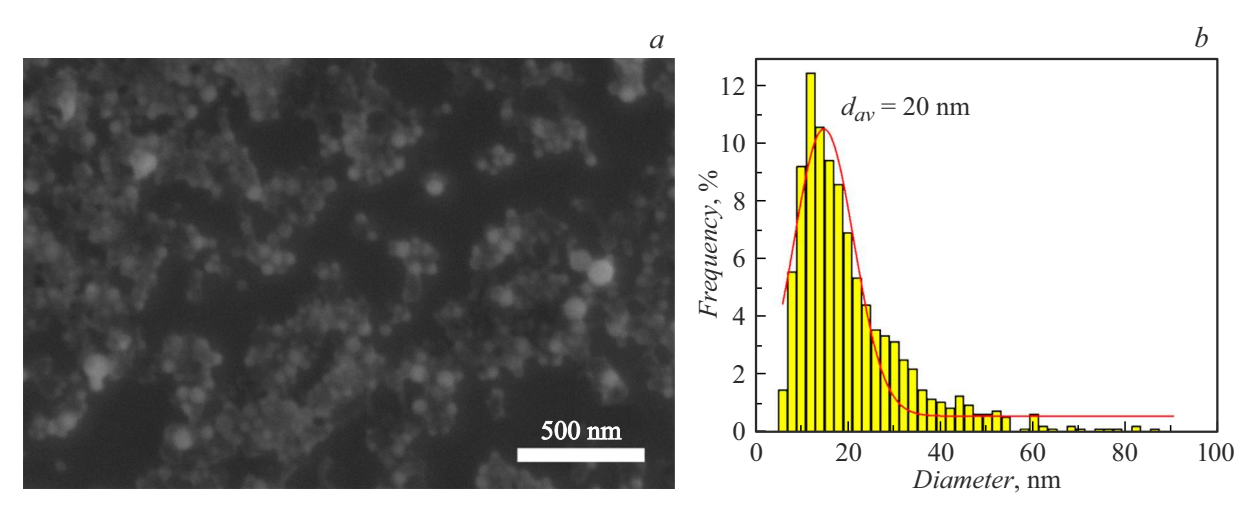
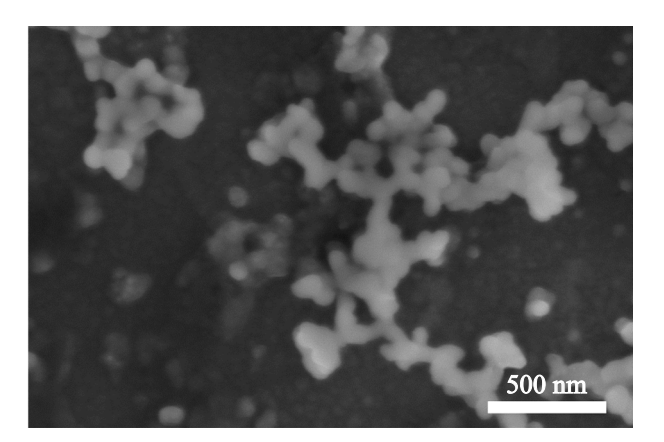


Figure 6. SEM image of (a) and the histogram of size distribution of the nanoparticles (b) that are produced as a result of fragmentation in ethanol for 20min.



**Figure 7.** SEM image of the nanoparticles produced as a result of fragmentation in acetone for 70 min.

Fig. 6 shows the SEM images of the nanoparticles produced as a result of laser fragmentation in ethanol for 20 min and the histogram of size distribution of the nanoparticles.

As a result of laser fragmentation in ethanol for 20 min, there is decrease of the average size of the nanoparticles to 20 nm. In case of acetone, the SEM images of the nanoparticles after laser fragmentation for 60 min exhibit larger nanoparticles (Fig. 7) than before laser irradiation, which can be related to melting of the particles in interaction with laser radiation and high contribution of the solvent (acetone). When comparing dynamics of change of the optical properties of the solution and the color, it can be state that the process proceeds much more slowly. After 70 min of laser radiation, the solution has a gray-bluish shade and there are explicitly signs of sedimentation. With centrifugation at 9660 g for 15 min, a supernate liquid has a pale-light blue shade.

Fig. 8 shows the Raman scattering spectra for the nanoparticles produced as a result of laser fragmentation

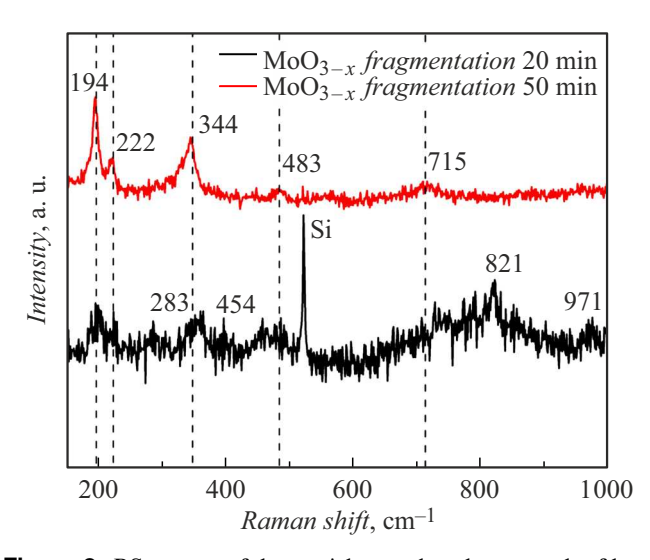


**Figure 8.** RS spectra of the particles produced as a result of laser fragmentation of the colloidal solutions in ethanol for 20 (the black line) and 50 min (the red line).

of the colloidal solutions in the ethanol medium for 20 and 50 minutes.

Based on the obtained Raman scattering spectra, it is clear that the study of the particles produced as a result of laser fragmentation for 20 min has not peaks that are typical for MoS<sub>2</sub>, thereby indicating the change of the chemical composition. There is a number of the peaks observed at 194, 222, 283, 344, 454, 483, 715, 821, 971 cm<sup>-1</sup>. In case of increase of the fragmentation time to 50 min, the peaks at 283, 454, 821 and 971 cm<sup>-1</sup> are not observed. In both the cases, the nanoparticles oxidize to result in formation of molybdenum oxide with oxygen vacancies [19].

Fig. 9 shows the Raman scattering spectra for the nanoparticles produced as a result of laser fragmentation of the colloidal solutions in the acetone medium for 60 minutes.

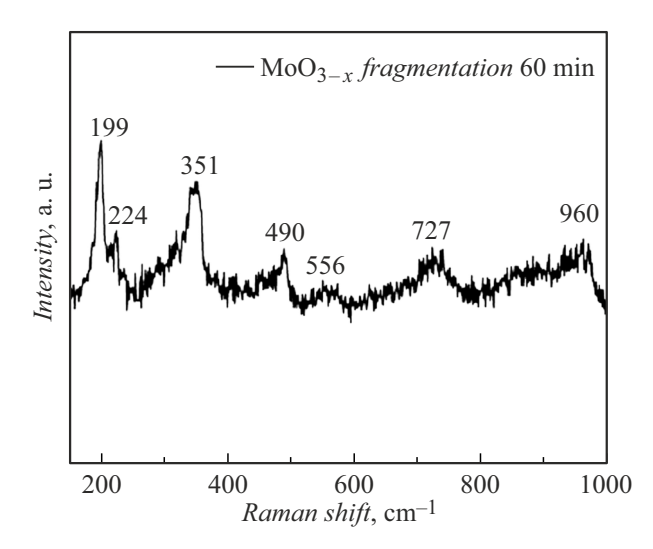


**Figure 9.** RS spectra of the particles produced as a result of laser fragmentation of the colloidal solutions in acetone for 60 min

The peaks at 199, 224, 351, 490 and  $727 \,\mathrm{cm}^{-1}$  are typical for substoichiometric  $\mathrm{MoO}_{3-x}$ . Thus, we can say that during the process of laser irradiation of the  $\mathrm{MoS}_2$  colloidal solution in acetone the nanoparticles are oxidized, thereby resulting in formation of molybdenum oxide with the oxygen vacancies [19].

# Photothermal properties of the colloidal solutions of molybdenum oxide and molybdenum disulfide

The optical properties of the synthesized colloidal solutions of the nanoparticles were studied by means of the spectrophotometer SF-2000 within the range 400-1000 nm using the quartz cuvettes with the optical path length of 10 mm. Fig. 10 shows the spectra of the optical density of the solution of the  $MoS_2$  nanoparticles and the  $MoO_{3-x}$  nanoparticles (fragmentation for 50 min) in ethanol.

Due to origination of the absorption peaks within the range 760–840 nm on the optical spectra of the colloidal solutions after laser fragmentation, the further stage of the study was measurement of a photothermal response using an additional installation. Laser radiation at the wavelength of 805 nm with the average power of 0.75 W was transmitted through the quartz cuvette with the colloidal solution. The transmitted radiation was recorded by a power meter. A thermal imager was used to detect variation of the temperature of the solutions with laser irradiation every 10 s for 10 min with subsequent cooling (10 min). The graphs of the dependences of variation of the temperature on the irradiation time and of the power of transmitted radiation on time are shown in Fig. 11.

With irradiation of the solution of the  $MoS_2$  nanoparticles the temperature increased from 22.5 °C to 40.1 °C (increase by 17.6 °C). In case of irradiation of the  $MoO_{3-x}$ 

nanoparticles, the temperature increased from 22.5 °C to 42.5 °C (increase by 20 °C). The materials based on molybdenum disulfide and molybdenum oxide absorb in the near-IR range, thereby making them quite effective for conversion of light energy into heat energy. The  $MoO_{3-x}$ nanoparticles have pronounced absorption peaks within the range 600-850 nm, which is related to structural specific features of the material [20]. At this, molybdenum oxide is a material that is more resistant to higher temperatures, which is important for photothermal applications, while the nanoparticles based on molybdenum disulfide oxidize over time. After laser fragmentation, the synthesized  $MoO_{3-x}$ have a smaller size, which also affects the rate of heating and cooling during photothermia. Molybdenum oxide is less toxic as compared to molybdenum disulfide, thereby making it more preferable for being used in biomedical and environmental applications [21].

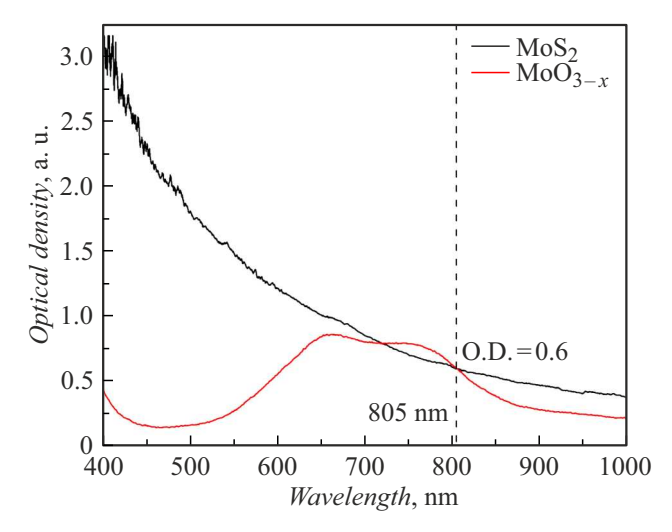


**Figure 10.** Spectra of the optical density of the solution of the  $MoS_2$  nanoparticles (the black line) and the  $MoO_{3-x}$  nanoparticles in ethanol (the red line, fragmentation for 50 min).

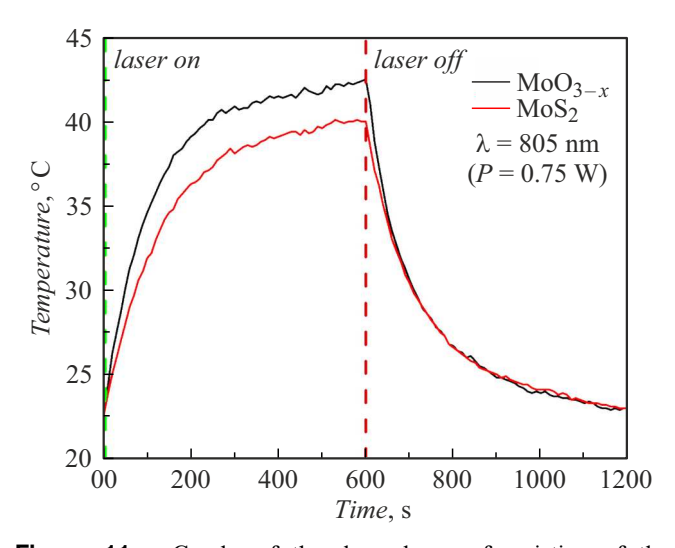


**Figure 11.** Graphs of the dependence of variation of the temperature of the produced solutions on the irradiation time.

# Conclusion

We have studied the influence of the parameters of femtosecond laser ablation and fragmentation in ethanol and acetone on the sizes and the composition of the nanoparticles. At the same time, the average sizes of the produced nanoparticles were about 36 nm in ethanol and 57 nm in acetone. Using the laser ablation method allows reducing the size of the nanoparticles to 20 nm, but with increase of the treatment time the produced nanoparticles oxidize, which can be related to formation of defects in the nanoparticles and dissociation of solvent molecules. The MoS<sub>2</sub>-based nanoparticles can absorb various biomolecules and drug molecules by covalent or noncovalent interactions. Using laser radiation, it is possible to produce the various types of the nanoparticles and their modifications, thereby improving tumor targeting and colloidal stability as well as accuracy and sensitivity for detecting specific biomarkers. At the same time, in the near-infrared region (600-850 nm)the MoO<sub>3-x</sub> nanoparticles have the pronounced absorption peaks and high efficiency of photothermal conversion, thereby making it possible to carry out phototherapy. The change of the temperature of the solutions during laser irradiation for 10 min allowed increasing the temperature of the solutions by 17.6 °C for the MoS<sub>2</sub> nanoparticles and by 20 °C for the MoO<sub>3-x</sub> nanoparticles.

## **Funding**

The study of laser ablation processes for formation of photosensitized nanoparticles and their characterization for theranostics was conducted using the grant of the Russian Science Foundation № 22-79-10348. The study of the processes of energy conversion and control of spectral characteristics of the nanoparticles was carried out using the grant of the Russian Science Foundation № 24-12-20015. The experimental diagrams were designed under the state assignment for research from the Ministry of Science and Higher Education of the Russian Federation (the topic FZUN-2024-0018, the state assignment of Vladimir State University).

#### Conflict of interest

The authors declare that they have no conflict of interest.

## References

- A. Abareshi, N. Salehi. J. Mater. Sci: Mater. Electron., 33, 25153 (2022). DOI: 10.1007/s10854-022-09220-7
- [2] A.B. Bucharskaya, N.G. Khlebtsov, B.N. Khlebtsov, G.N. Maslyakova, N.A. Navolokin, V.D. Genin, E.A. Genina, V.V. Tuchin. Materials, 15 (4), 1606 (2022). DOI: 10.3390/ma15041606
- [3] Y. Bayazitoglu, S. Kheradmand, T.K. Tullius. Int. J. Heat Mass Transf., 67, 469 (2013).DOI: 10.1016/j.ijheatmasstransfer.2013.08.018

- [4] J. Wang, L. Sui, J. Huang, L. Miao, Y. Nie, K. Wang, Z. Yang, Q. Huang, X. Gong, Y. Nan, K. Ai. Bioact. Mater., 6 (11), 4209 (2021). DOI: 10.1016/j.bioactmat.2021.04.021
- [5] K. Bazaka, I. Levchenko, J.W.M. Lim, O. Baranov, C. Corbella, S. Xu, M. Keidar. J. Phys. D: Appl. Phys., 52 (18), 183001 (2019). DOI: 10.1088/1361-6463/ab03b3
- [6] L. Ding, Y. Chang, P. Yang, W. Gao, M. Sun, Y. Bie, L. Yang, X. Ma, Y. Guo. Mater. Sci. Eng. C, 117, 111371 (2020). DOI: 10.1016/j.msec.2020.111371
- [7] U.E. Kurilova, A.S. Chernikov, D.A. Kochuev, L.S. Volkova, A.A. Voznesenskaya, R.V. Chkalov, D.V. Abramov, A.V. Kazak, I.A. Suetina, M.V. Mezentseva, L.I. Russu, A.Yu. Gerasimenko, K.S. Khorkov. J. Biomed. Photonics Eng., 9 (2), 020301 (2023). DOI: 10.18287/JBPE23.09.020301
- [8] U.E. Kurilova, A.S. Chernikov, D.A. Kochuev, L.S. Volkova, A.A. Voznesenskaya, R.V. Chkalov, D.V. Abramov, A.V. Kazak, I.A. Suetina, M.V. Mezentseva, L.I. Russu, A.Yu. Gerasimenko, K.S. Khor'kov. Biomed. Eng., 58, 106 (2024). DOI: 10.1007/s10527-024-10376-1
- [9] C.L. Lai, R. Karmakar, Y.M. Tsao, S.C. Lu, A. Mukundan, P.H. Liu, H.C. Wang. Opt. Mater. Express, 14 (8), 2003 (2024). DOI: 10.1364/OME.528709
- [10] Q. Li, J.T. Newberg, E.C. Walter, J.C. Hemminger, R.M. Penner. Nano Lett., 4 (2), 277 (2004). DOI: 10.1021/nl035011f
- [11] U. Krishnan, M. Kaur, K. Singh, M. Kumar, A. Kumar. Superlattice. Microst., 128, 274 (2019). DOI: 10.1016/j.spmi.2019.02.005
- [12] A.S. Chernikov, G.I. Tselikov, M.Yu. Gubin, A.V. Shesterikov, K.S. Khorkov, A.V. Syuy, G.A. Ermolaev, I.S. Kazantsev, R.I. Romanov, A.M. Markeev, A.A. Popov, G.V. Tikhonowski, O.O. Kapitanova, D.A. Kochuev, A.Yu. Leksin, D.I. Tselikov, A.V. Arsenin, A.V. Kabashin, V.S. Volkov, A.V. Prokhorov. J. Mater. Chem. C, 11 (10), 3493 (2023). https://doi.org/10.1039/D2TC05235K
- [13] G.I. Tselikov, D.A. Panova, I.S. Kazantsev, A.V. Syuy, G.V. Tikhonowski, A.A. Popov, A.V. Arsenin, V.S. Volkov. Bull. Russ. Acad. Sci. Phys., 86 (Suppl 1), S234 (2022). DOI: 10.3103/S1062873822700745
- [14] B. Guo, J. Sun, Y. Hua, N. Zhan, J. Jia, K. Chu, Nanomanuf. Metrol., 3, 26 (2020). DOI: 10.1007/s41871-020-00056-5
- [15] A.A. Ionin, S.I. Kudryashov, A.A. Samokhin. Phys. Usp., 60, 149 (2017). DOI: 10.3367/UFNe.2016.09.037974
- [16] G. Bongiovanni, P.K. Olshin, C. Yan, J.M. Voss, M. Drabbels,
  U.J. Lorenz. Nanoscale Adv., 3 (18), 5277 (2021).
  DOI: 10.1039/D1NA00406A
- [17] R. Fang, A. Vorobyev, C. Guo. Light Sci. Appl., 6, e16256 (2017). DOI: 10.1038/lsa.2016.256
- [18] A.V. Kharkova, A.A. Voznesenskaya, D.A. Kochuev, K.S. Khorkov. Bull. Russ. Acad. Sci.: Phys., 86(6), 726 (2022). DOI: 10.3103/S1062873822060156
- [19] F. Ye, D. Chang, A. Ayub, K. Ibrahim, A. Shahin, R. Karimi, S.Wettig, J. Sanderson, K.P. Musselman. Chem. Mater., 33 (12), 4510 (2021). DOI: 10.1021/acs.chemmater.1c00732
- [20] J. G. Castillo-Lara, N. Zamora-Romero, K. Isaac-Olive, N.P. Jiménez-Mancilla, L. Aranda-Lara, S. Camacho-López, M. Camacho-López,, A.R. Vilchis-Nestor, M.A. Camacho-López. Mater. Lett., 388, 138300 (2025). DOI: 10.1016/j.matlet.2025.138300

Translated by M.Shevelev